A Compact Radio-Frequency Power Supply for Ion and Particle Guides and Traps

Ivo Cermak
Fakultät für Naturwissenschaften, Technische Universität Chemnitz,
D-09107 Chemnitz, Federal Republic of Germany

mailto:ivo.cermak@physik.tu-chemnitz.de

(Received:

Abstract

In this paper, we present a novel compact rf or ac power generator that uses a resonant driving scheme without the necessity for any matching device. The developed unit also doesn't need any expensive high voltage power supply for generating output voltages in the range of some hundred volts typically required for the function of trapping devices. The high efficiency of the generator allows operation at output powers of around 50 W without any performance losses. The frequency range of the device is determined by the output transformer. It can be easily varied from the megahertz range down to some kilohertz just by replacing the output transformer and several capacitors in the control part of the generator. Thus, our device can be used for supplying traps operating with ions as well as with charged nano- or microparticles.

PACS numbers: 84.30.Ng, 82.80.Ms, 29.30.Aj, 07.75.+h, 07.81.+a

I. Introduction

Electrode arrangements powered by radio frequencies are widely used for guiding or trapping ions, nano- or microparticles. The shapes of such devices range from three-dimensional quadrupoles (Paul-traps), linear quadrupoles and octopoles, to multipole devices such as 22-pole or ring-electrode traps.[1, 2]

The operation frequency depends on the charge q and mass m of the particles that should be guided or trapped. As an example, we consider operation of a linear (2D) multipole trapping device with $2n$ poles located at a radius r_0 and supplied with rf-voltage with the amplitude V_0 and frequency $\Omega = 2\pi f$: $V(t) = V_0 \cdot \sin(\Omega t)$. The electrostatic potential in the multipole is given in cylindrical coordinates by the formula $\Phi = \hat{r}^n \cdot \cos(n\varphi) \cdot V_0 \cdot \sin(\Omega t)$, where $\hat{r}$ is the reduced radius $\hat{r} = r/r_0$.[1, 2] Charged particles will be trapped in an effective potential

$$V_{eff} = \frac{n^2}{4} \frac{V_0^2}{r_0^2 \Omega^2} \cdot \frac{q^2}{m} \cdot \hat{r}^{2n-2}.$$

The trapping properties of radio-frequency traps are characterized by the adiabaticity parameter η. For safe operation, this parameter must be lower than 0.3. The adiabaticity parameter for multipole devices can be calculated from the following formula (see also Ref. 1 or 2):

$$\eta = 2n(n-1)\cdot\frac{V_0}{r_0^2\Omega^2}\cdot\frac{q}{m}\cdot\hat{r}^{\,n-2}.$$

The operation of an rf trapping device with single-charged ions ($q = e_0$) will be limited at the low-mass range by the adiabaticity and at the high-mass range by the depth of the effective potential. When operation with single-charged ions with a mass range extending from m_{min} to m_{max} and kinetic energies up to E_m is required, the following conditions must be fulfilled:

$$\eta(m_{\min}) < 0.3$$

$$V_{eff}(m_{\max}) \geq E_m$$

From these conditions, a requirement for the amplitude of the supply voltage V_0 can be derived

$$\frac{2}{n\cdot\hat{r}^{\,n-1}}\sqrt{E_m}\,\frac{\sqrt{m_{\max}}}{e_0}\,r_0\Omega < \frac{3}{20}\cdot\frac{r_0^2\Omega^2}{n(n-1)\cdot\hat{r}^{\,n-2}}\cdot\frac{m_{\min}}{e_0}.$$

This condition is fulfilled when

$$\Omega > \Omega_{\min} = \frac{40(n-1)}{3\hat{r}}\cdot\frac{\sqrt{E_m}}{r_0}\cdot\frac{\sqrt{m_{\max}}}{m_{\min}}.$$

A numerical formula can be derived for practical usage:

$$f > f_{\min} = 2.08\,\mathrm{MHz}\cdot\frac{n-1}{\hat{r}}\cdot\frac{\sqrt{E_m/\mathrm{eV}}}{(r_0/\mathrm{cm})^2}\cdot\frac{\sqrt{m_{\max}/\mathrm{u}}}{m_{\min}/\mathrm{u}} \qquad (1)$$

When the frequency of the supply voltage is set to $f = f_{\min}$, the amplitude of the necessary supply voltage can be obtained:

$$V_0 = \frac{80(n-1)}{3n\cdot\hat{r}^{\,n}}\cdot\frac{E_m}{e_0}\cdot\frac{m_{\max}}{m_{\min}} \qquad (2)$$

From these formulas, the operation frequencies and voltages can be obtained (see Table 1). The highest operational frequencies are required for fragmentation studies, where extremely high effective potentials are needed (see 2nd and 3rd column of Table 1). For experiments with thermalized ions, the operational parameters depend on the trap type and the expected ion temperature. The frequencies vary from typically 10 to 20 MHz for protons, several MHz for heavier ions, to less than 1 MHz for large ions like C_{60}^+. Even heavier species, such as large ion clusters, nano, or microparticles, require much lower operation frequencies down to the audio (af) range. Weakly charged microparticles can be stored in a quadrupole trap operated with frequencies as low as 50 Hz.

Several driving methods are used for supplying the trapping devices. Whereas direct drive by an amplifier is a suitable solution for operation at lower frequencies (see e.g. Ref. 3), the power needed for driving the trap capacitance limits the use of such a driving scheme for higher frequencies. We assume a trap with capacitance C that is driven in a two-phase mode by the total voltage $V(t) = 2V_0 \cdot \sin(\Omega t)$. The supply current $I(t) = \Omega C \cdot 2V_0 \cdot \cos(\Omega t)$ is provided by a two-channel amplifier using dc supply voltages $\pm V_M$. If losses in the cables can be neglected, the required supply power is given by the power dissipated in both channels of the driving amplifier. The mean value of this quantity amounts to

$$P_{Diss} = 2 \cdot \frac{2}{T} \int_{-T/4}^{T/4} (V_M - V(t)/2) \cdot I(t) \cdot dt$$

where $T = 1/f$ is the period of the supply voltage. For the given example, the total dissipated power is $P_{Diss} = 16 f \cdot C \cdot V_0 \cdot V_M$. The highest efficiency we get at the maximum possible output voltage $V_0 = V_M$ where the dissipated power reaches the value

$$P_{Diss} = 16 f \cdot C \cdot V_0^2 .$$

For trap capacitance C = 100 pF and ac-voltage with amplitude V_0 = 500 V, the dissipated power would reach 100 W already at an operating frequency f = 250 kHz.

To overcome the power problem at higher frequencies, the trapping devices are operated as a part of a resonance circuit. In the ideal case, the required supply power equals to the power dissipated in the resonant circuit. The latter is given just by the losses in the real resonance circuit given by the power dissipated on the circuit's resistance. Under the same driving conditions as in the previous example, the dissipated power amounts to

$$P_{Diss} = \frac{4\pi f C V_0^2}{Q} .$$

Compared to direct drive, this scheme reduces the dissipated power by a factor of $4Q/\pi$. An additional advantage is the low distortion of the driving voltage due to higher harmonics given by the filtering properties of the resonance circuit. A minor drawback of the resonant supply is the need for a matching network. This circuitry transforms the high impedance of the resonant circuit to the standard 50 Ω output impedance of commercial generators. The adjustment of the network is crucial for reaching a sufficiently low amount of reflected power. When a trapping device with variable temperature range is used, a readjustment at different operating temperatures might be necessary. Nevertheless, even a properly adjusted matching network is a source of additional power losses.

The resonant driving scheme can be used without any matching device. The resonant circuit is a part of the driving device that acts as an oscillator (see for instance Ref. 4). Our power generator uses a similar driving method. However, we applied modern electronic components, which resulted in a cheap, compact construction with high output power and efficiency.

II. Design

The principle schematic of the generator is shown in Fig. 1. The circuitry is similar to those used in resonant switching power supply units. The crucial difference from commercial power supply units is the much higher available operating frequency of our design. The radio-frequency output voltage of the generator is generated by the transformer TR1. The transformer is driven by a symmetrical push-pull power stage consisting of two power MOS-FETs T1 and T2. The supply voltage for the power stage is provided by an external power supply unit (PSU). The control signals for switching the power stage are derived from two monostable flip-flop circuits (monoflops) and two drivers from output signals of an externally synchronized oscillator. The width of the control pulses together with the magnitude of the supply voltage determines the amount of energy that is accumulated in the output transformer during each half cycle of the output signal, thereby influencing the amplitude of the generator's output voltage. The output voltage can be shifted by applying an auxiliary dc voltage Vo via a coil Lo that is connected to the center of the resonant circuit and which acts as a low pass filter.

The output transformer TR1 directly supplies the trapping device, which behaves as the capacitive part of a resonance circuit. The design of the transformer is crucial for the function of the whole generator. Usually, the inductance of the secondary coil should be substantially higher than the inductance L of the connected resonant circuit. The conversion ratio of the transformer determines the effective resistive load of the resonant circuit during the switch-on time of the power stage. When sufficiently high conversion ratio is selected, the generator will not affect the function of the resonant circuit and a high quality value can be reached. Since the primary coil of the transformer is supplied by a relatively low voltage (typically less than 50 V), high peak currents may result in magnetic saturation of the core material. The core material and the size must be chosen according to the operating frequency, output and supply voltages, and according to the required output power.

The external resonance circuit determines the operating frequency of the generator. For proper function, the free running frequency of the generator's oscillator should be set to a slightly lower value than the resonant frequency. The feedback via two resistors and delay elements ensures that the generator will lock to the resonant frequency. The magnitude of the delay of both elements is substantial for proper locking and for reaching an appropriate phase matching between the output voltage of the generator and the control signals that drive the power stage. The delays of both elements must be adjusted according to the operating frequency and according to the parameters of the power stage and the output transformer.

The oscillator can be stopped by grounding an external TTL input (Enable). This results in a shut down of the generator, and the external resonant circuit connected to the generator output will perform free damped oscillations. This will cause an exponential decay of the amplitude of the output voltage, $V_0(t) = V_0 \exp(-t/\tau)$ with a time constant τ that depends on the quality Q of the resonant circuit:

$$\tau = \frac{\sqrt{4Q^2 - 1}}{\Omega}.$$

In practice, the decay to half amplitude can be approximated by $\tau_{1/2} \approx T \cdot Q / 4.5$, where T is the period of the output signal.

The amplitude of the output voltage of the generator is determined by the magnitude of the supply voltage. A properly stabilized PSU with sufficiently high output power should be used. Any low-frequency instabilities of the supply voltage would directly influence the amplitude of the output voltage, thus resulting in losses of performance of the connected trapping device. A computer controlled PSU can be easily used to program the output voltage. Together with the digital input for turning off the generator (Enable), it offers a variety of possibilities for controlling the output voltage of the generator.

The electronic schematic of the generator is shown on Fig. 2. Several integrated circuits are used to fulfill the functions of the blocks from Fig. 1: IC2 is the oscillator with external synchronization, IC1 the delay elements, IC3 fulfils the function of both monoflops, and IC4 to IC7 of the drivers of the power MOS-FETs. To reach high switching speed, integrated circuits of the AC-MOS and HC-MOS families[5] and fast power MOS-FETs[6] were used. The design requires an auxiliary power supply (IC8) that provides supply voltages for the oscillator and supplies the power required to drive the power stage.

The oscillator is a standard design of a three-inverter circuitry with one RC delay element. If the synchronization inputs 1 and 5 of the NAND gates IC2a and b are set to logical 1, all three NAND gates IC2a, b and c behave as inverters and the oscillator is free running. The output waveform has a duty factor of nearly 50% and a frequency given by the time constant R7·C5 of the delay element, which can be easily adjusted over a wide range.

The synchronization of the oscillator is attained by applying negative logical signals to the control inputs 1 and 5 of the gates IC2a and b, respectively. The logical 0 on either input stops the current half period of the oscillations, thus resulting in synchronization of the oscillation frequency with the frequency of the applied signal. The synchronization signals are gained by digitizing and delaying the output voltage of the generator. The output voltage from the transformer TR1 is fed via two pairs of resistors R10-13 to the high pass filters C1 R1 and C2 R2. The filters suppress the DC component of the output voltage and the output signals are digitized by the Schmitt trigger gates IC1a and d. The next RC elements (R5 C3 and R6 C4) together with the subsequent Schmitt trigger gates IC1b and c introduce a settable delay to achieve proper phase matching.

The output pulses from the oscillator are processed in a pulse shaper. The pulse shaper possesses two identical channels (monoflops), each consisting of a delay element (R8 C6 and R9 C7) and two gates (IC3a, d and IC3b, c). The output NOR gates (IC3d and IC3c) produce positive pulses as a response to falling slopes of the input signals. The length of the pulses is given approximately by the time constant of the corresponding RC element and the propagation delay in the inverter (IC3a and IC3b).

Each of the pulse signals is fed via 16 parallel connected buffers (IC4, 5 and IC6, 7) to the corresponding power MOS-FET (T1 and T2) of the power stage. The parallel connection of the buffers allows the high driving capability necessary for fast switching of the power MOS-FET.

A digital signal at the input CN5 can be used to turn off the generator. When the input is grounded, the inputs 1 and 12 of the gates IC1a and d will be set to logical 0. The oscillator will be stopped, the outputs of the pulse shaper will be set to logical 0, too, and the power stage will be turned off.

The generator requires two separate supply voltages - one for the driving circuitry and another for the output stage. The external supply voltage for the output stage is connected to the sockets CN3 and CN4 and decoupled by a set of capacitors C23-C28. The voltage for the driving circuitry is produced from the mains (CN1) by the transformer TR2. The secondary voltage is rectified (diodes D1, 2) and filtered (C8).

The voltage regulator IC8 provides a stabilized voltage of 6 V supplying the logic ICs. The decoupling capacitors C12-22 increase the stability of the circuit. The output voltage of the regulator is shifted by three diodes D3-5 such that the supply voltages of the logic ICs (Vdd and Vss) reach values of approximately +8 V and +2 V respectively. These voltages also determine the magnitude of the control signals of the power stage. The values of the supply voltages were chosen so that the switching properties of the logical ICs and of the MOS-FETs of the power stage would be optimized.

The major parts of the generator's electronics were placed onto a printed circuit board and, together with the output transformer, fixed into an aluminum box of about $17\times11\times5$ cm^3 (Fig. 3). The box also provides the high-frequency shielding of the generator's signals. The front and rear plates hold the BNC connectors for the signal output and the digital control for turning off the generator, connectors for the external power supply, and the main plug (Fig. 4). One side of the box is used to cool the MOS-FETs of the power stage and the voltage regulator IC8. An external aluminum radiator and a fan are used to support the cooling. The whole unit is mounted on a metallic plate, which is fixed on the vacuum flange to which the trapping device is attached. This compact construction allows for short connection cables with low capacity.

III. Performance

The operation of the generator has been tested at several working frequencies in the megahertz range. We used the device for supplying our ring electrode trap (see e.g. Ref. 1) at frequencies of about 4.2, 5.6, and 7.8 MHz. The coil L of the external resonant circuit is permanently connected to the trapping device. The operation frequencies were changed by connecting one or two external 1 nF capacitors, in a parallel or serial connection between each trap electrode and the ground. To achieve the best performance, the settable elements of the generator were adjusted to the optimal values given in Table 2. Another application of our device was supplying of linear quadrupole, where output voltages with amplitudes up to about one kilovolt and frequencies around 1 MHz were required. For this operation mode, an external resonant circuit was built using of a coil with an inductance of about 70 µH (50 turns at a diameter of 50 mm, total coil length: 100 mm). By tuning the external capacity, the resonance frequency was set to 1 MHz. The optimal values of the settable elements can be found in Table 2.

Figures 5 and 6 illustrate the function of the generator at the operating frequency of 5.6 MHz. Figure 5 shows the dependence of the amplitude of the output voltage on the supply voltage. Since the device was for this application designed for higher operating voltages and powers, the internal oscillator starts to lose synchronization at output voltages lower than about 80 V. Operation down to about 10-20 V rf amplitude is possible, but is accompanied by a non-linear dependence on the supply voltage and minor changes of the operation frequency.

The dependence of the supply power and of the output power on the output voltage is depicted on Figure 6. The figure also shows the calculated efficiency. We measured the quality of the connected resonant circuit from the decay of the output signal (see above). The output power was calculated from the quality and from the estimated total capacity of the circuit. The comparatively low inductance of the external coil caused a low quality of the resonant circuit, thus requiring powers of around 50 W at operating voltages of amplitudes of 200 V on each trap electrode.

Figure 7 shows the frequency spectrum of the output signal. The spectrum was measured and calculated by the LeCroy LT342 oscilloscope. The spectrum indicates a clean sinusoidal signal. Despite some weak high-frequency noise, there is no visible contribution due to harmonic or sub-harmonic frequencies.

IV. Conclusion

We presented a compact power generator that can be easily used for supplying ion and particle traps. The unit was routinely used for driving our ring-electrode trap at frequencies varying from 4 to 8 MHz. In this application, the generator was supplying output power up to about 50 W. The examples shown in the previous section demonstrate the operation also at lower frequencies. One of the possible applications is the driving of a quadrupole mass filter. The stability of the output voltage and frequency predetermine the generator as a part of a low-cost mass filter with resolution power not exceeding one hundred. The operational frequency can be scaled down to the kilohertz range by using a suitable output transformer. At such operation conditions, the generator can be used for supplying nano- and microparticle traps.

Acknowledgment

The development of the generator was supported by the DFG within Project 7: *Growth Dynamics of Carbon-Containing Nanostructures* of the Forschergruppe *Laboratory Astrophysics*.

References

[1] D. Gerlich, "Inhomogeneous RF Fields: A Versatile Tool for the Study of Processes with Slow Ions" in State-Selected and State-to-State Ion-Molecule Reaction Dynamics, Part 1, edited by C.-Y. Ng and M. Baer (Adv. in Chem. Phys. Series), Vol. LXXXII, 1-176 (1992).

[2] D. Gerlich, "Rf Ion Guides" in The Encyclopedia of Mass Spectrometry, edited by P. B. Armentrout (Elsevier Ltd., 2003), Vol. 1, 182-194, ISBN 0-08-043802-4.

[3] I. Cermak, E. Grün, and J. Svestka, "New Results in Studies of Electric Charging of Dust Particles," Adv. Space Res. 15, #10, 59 (1995).

[4] R. M. Jones, D. Gerlich, and S. L. Anderson, "A Simple Radio-Frequency Power Source for Ion Guides and Ion Traps," Rev. Sci. Instrum. 68 (9), 3357-3362 (1997).

[5] Data sheets of the AC and HC logic families, e.g. http://www.onsemi.com/.

[6] Data sheets of Power MOSFET, http://www.irf.com/.

Tables

Table 1. Minimum values of the operating frequencies for multipole traps. The frequencies and the amplitudes of the supply voltages were calculated for the given maximum energies and ion types. For the calculation, the formulas (1) and (2) were used. In order to guarantee a safe operation, $\hat{r} = 0.8$ was taken. Since we supposed trapping of only one ion type (m_{min} = m_{max}), the required supply voltage doesn't depend on the ion mass.

Trap type	V_0 10 eV	f_{min} for H^+	V_0 100 meV	f_{min} for H^+	f_{min} for H_2^+	f_{min} for N_2^+	f_{min} for C_{60}^+
quadrupole, r_0 = 5 mm	208 V	16 MHz	2.1 V	1.6 MHz	1.2 MHz	0.31 MHz	61 kHz
octopole, r_0 = 5 mm	488 V	49 MHz	4.9 V	4.9 MHz	3.5 MHz	0.93 MHz	0.18 MHz
22-pole, r_0 = 5 mm	2822 V	165 MHz	28 V	16 MHz	12 MHz	3.1 MHz	0.61 MHz

Table 2. Optimal values of the settable elements

<table>
<tr><th>operating frequency</th><th>output transformer
TR1</th><th>oscillator frequency
C5</th><th>synchronization delay
C3, C4</th><th>control pulse duration
C6, C7</th></tr>
<tr><td>1 MHz</td><td>1 ferrite ring core:
ø61/35.6 mm×12.7 mm
(μ_r ≈ 2200, A_L = 3130 nH)
primary coil: 2×1 turn
secondary coil: 50 turns</td><td>330 pF</td><td>-</td><td>330 pF</td></tr>
<tr><td>4.2 MHz</td><td>4 ferrite ring cores:
ø29/19 mm×7.5 mm
(μ_r ≈ 120, A_L = 79 nH)
primary coil: 2×2 turns
secondary coil: 15 turns</td><td>47 pF</td><td>150 pF</td><td>470 pF</td></tr>
<tr><td>5.6 MHz</td><td rowspan="2">3 ferrite ring cores:
ø29/19mm×7.5 mm
(μ_r ≈ 120, A_L = 79 nH)
primary coil: 2×1 turn
secondary coil: 10 turns</td><td>33 pF</td><td>68 pF</td><td>220 pF</td></tr>
<tr><td>7.8 MHz</td><td>22 pF</td><td>-</td><td>100 pF</td></tr>
</table>

Figure Captions

FIG. 1. Principle schematic of the generator.

FIG. 2. Scheme of the generator.

FIG. 3. Inner assembly of the generator.

FIG. 4. Mechanic construction of the generator.

FIG. 5. Dependence of the amplitude of the generator output voltage on the supply voltage. The generator was supplying an external resonant circuit with resonant frequency of 5.6 MHz, parallel capacity of about 650 pF, and quality of 44. For the settings see also Table 2.

FIG. 6. Dependence of the input and output power and of the efficiency of the generator on the output voltage. For the operating parameters see Figure 5.

FIG. 7. Power spectrum of the generator output signal. The spectrum was taken at operating frequency of 5.6 MHz and amplitude of the output voltage of 170 V.

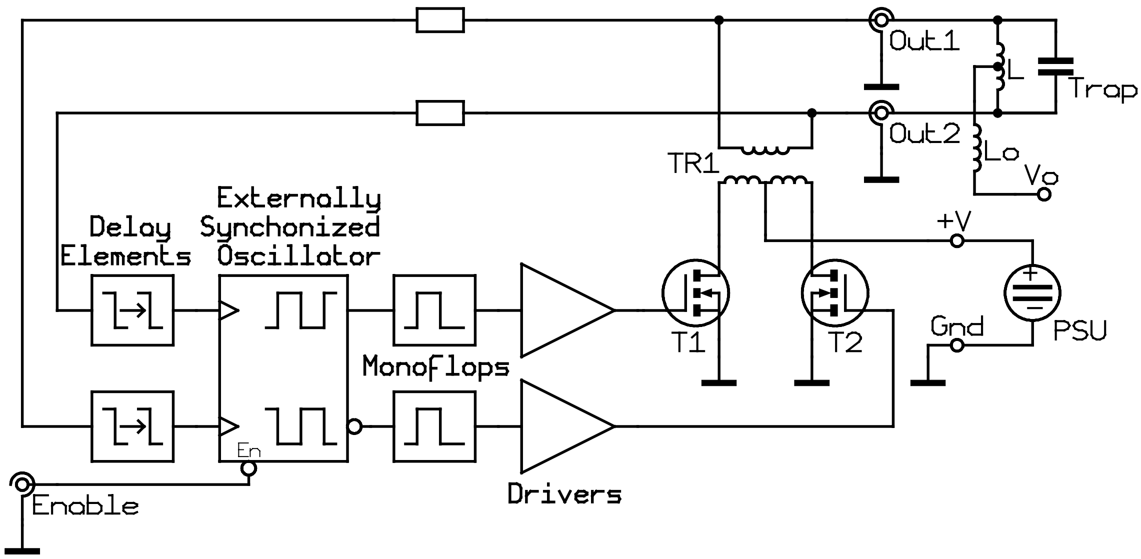
Out1
L
Trap
Out2
Lo
Vo
TR1
+V
Externally
Synchonized
Oscillator
Delay
Elements
T1
T2
PSU
Gnd
Monoflops
En
Enable
Drivers

FIG. 1.

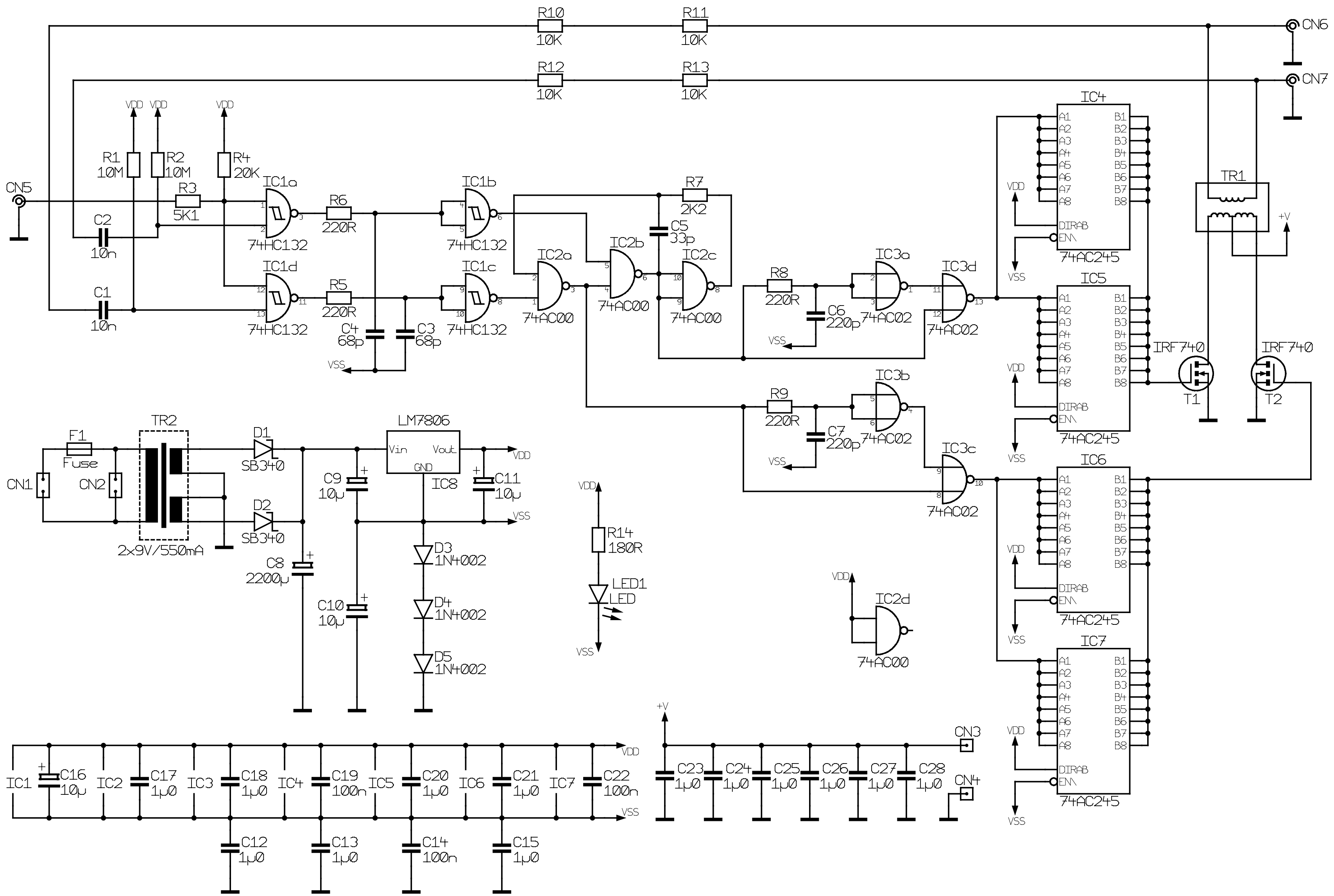
R10
10K
R11
10K
CN6
R12
10K
R13
10K
CN7
IC4
74AC245
IC5
74AC245
IC6
74AC245
IC7
74AC245
A1 A2 A3 A4 A5 A6 A7 A8
B1 B2 B3 B4 B5 B6 B7 B8
DIRAB
EN
TR1
+V
IRF740
T1
T2
VDD
VSS
R1
10M
R2
10M
R3
5K1
R4
20K
CN5
C2
10n
C1
10n
IC1a
IC1b
IC1c
IC1d
74HC132
R6
220R
R5
220R
C4
68p
C3
68p
R7
2K2
C5
33p
IC2a
IC2b
IC2c
IC2d
74AC00
R8
220R
C6
220p
R9
220R
C7
220p
IC3a
IC3b
IC3c
IC3d
74AC02
F1
Fuse
TR2
2x9V/550mA
CN1
CN2
D1
SB340
D2
SB340
C8
2200μ
C9
10μ
C10
10μ
LM7806
Vin
Vout
GND
IC8
C11
10μ
D3
1N4002
D4
1N4002
D5
1N4002
R14
180R
LED1
LED
IC1
C16
10μ
IC2
C17
1μ0
IC3
C18
1μ0
IC4
C19
100n
IC5
C20
1μ0
IC6
C21
1μ0
IC7
C22
100n
C12
1μ0
C13
1μ0
C14
100n
C15
1μ0
C23
1μ0
C24
1μ0
C25
1μ0
C26
1μ0
C27
1μ0
C28
1μ0
CN3
CN4

FIG. 2.

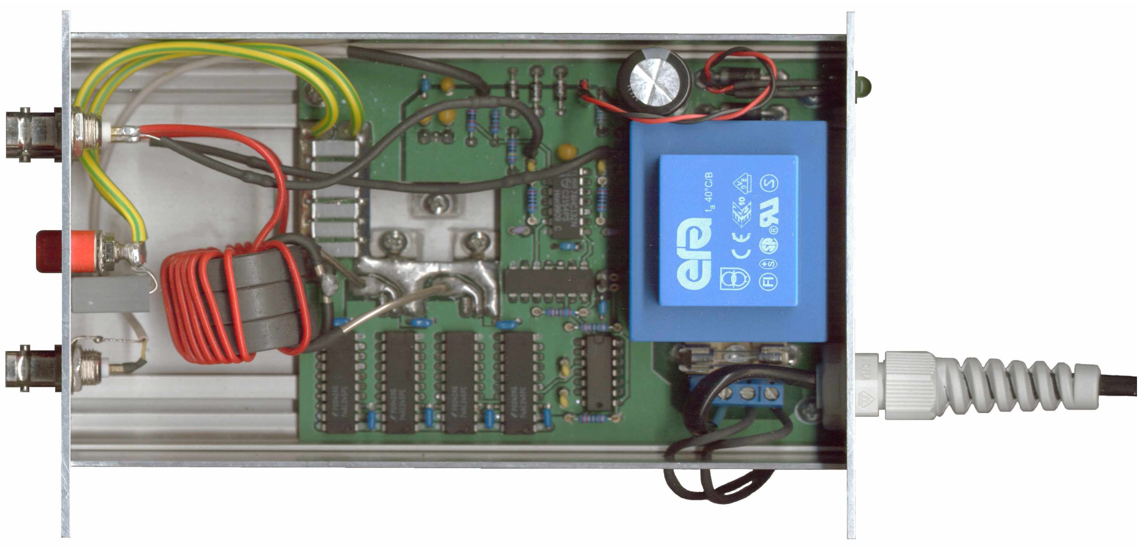

FIG. 3.

FIG. 4.

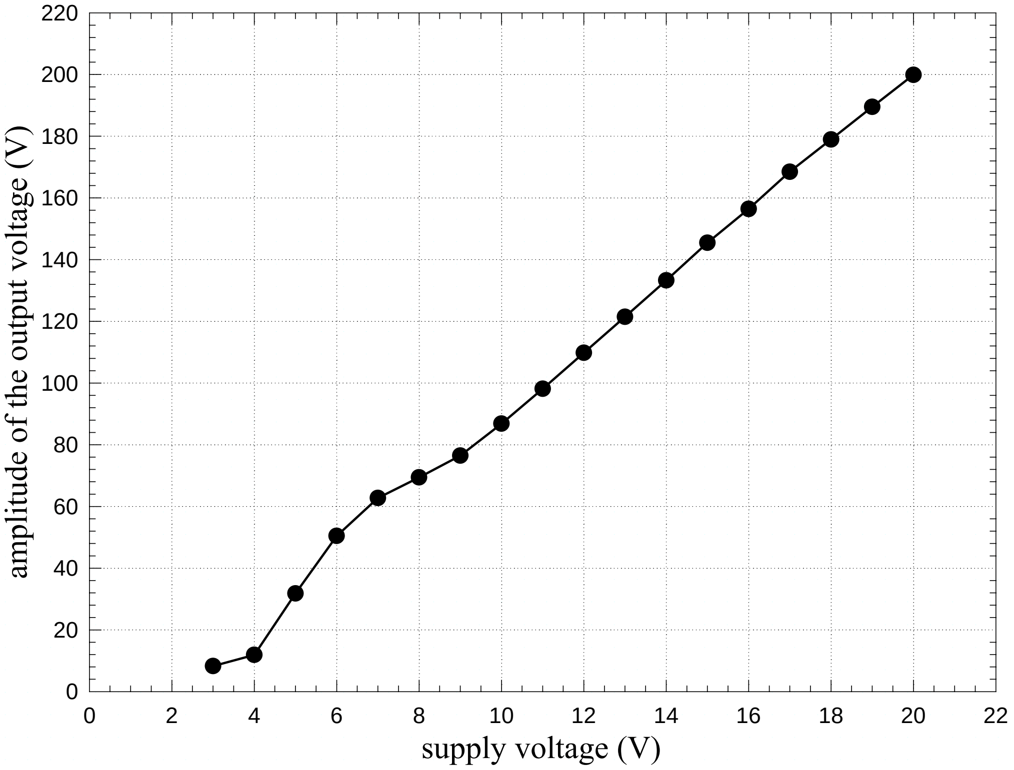
amplitude of the output voltage (V)
supply voltage (V)
0
20
40
60
80
100
120
140
160
180
200
220
0
2
4
6
8
10
12
14
16
18
20
22

FIG. 5.

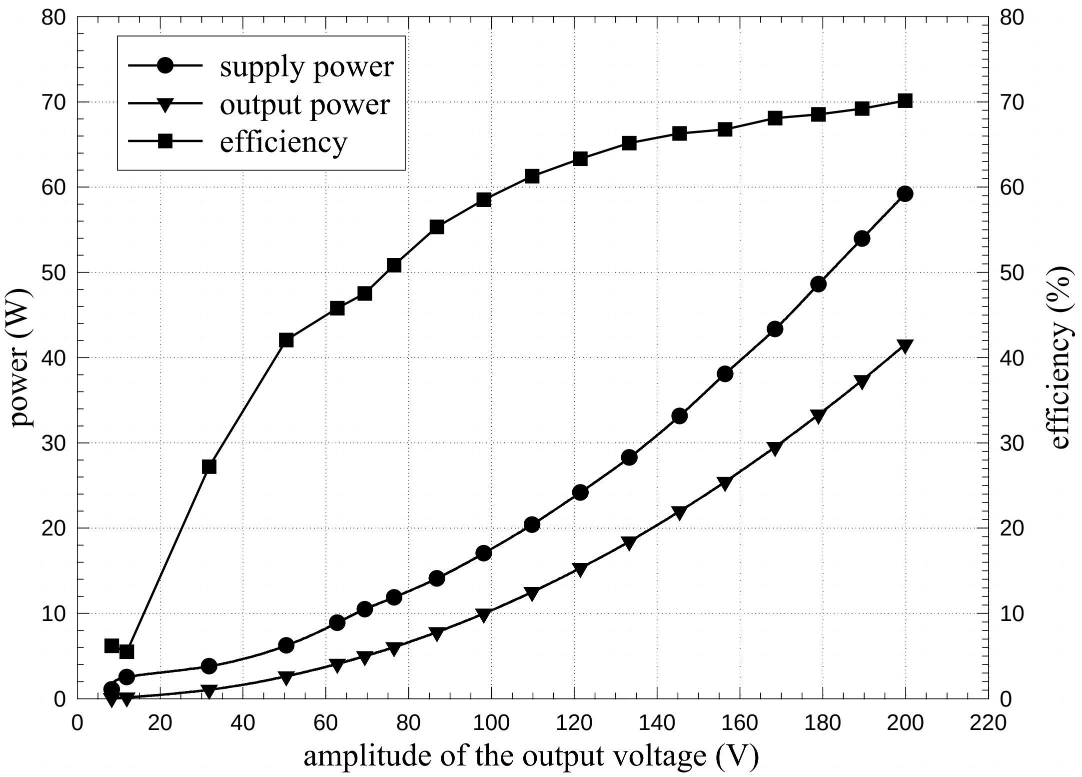
supply power
output power
efficiency
power (W)
efficiency (%)
amplitude of the output voltage (V)
0
10
20
30
40
50
60
70
80
0
20
40
60
80
100
120
140
160
180
200
220

FIG. 6.

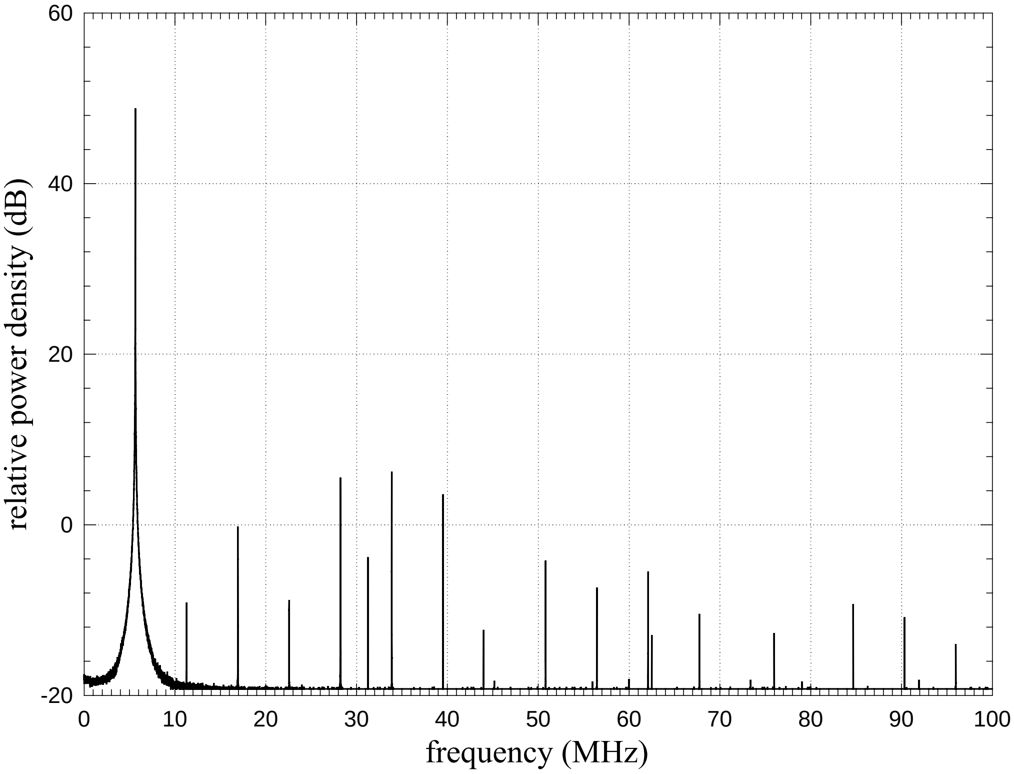
60
40
20
0
-20
relative power density (dB)
0
10
20
30
40
50
60
70
80
90
100
frequency (MHz)

FIG. 7.